Multi-target Track-Before-Detect using Labeled Random Finite Set

Francesco Papi[c], Ba-Tuong Vo[a], Mélanie Bocquel[b], Ba-Ngu Vo[a]

***Abstract*— Multi-target tracking requires the joint estimation of the number of target trajectories and their states from a sequence of observations. In low signal-to-noise ratio (SNR) scenarios, the poor detection probability and large number of false observations can greatly degrade the tracking performance. In this case an approach called Track-Before-Detect (TBD) that operates on the pre-detection signal, is needed. In this paper we present a labeled random finite set solution to the multi-target TBD problem. To the best of our knowledge this is the first provably Bayes optimal approach to multi-target tracking using image data. Simulation results using realistic radar-based TBD scenarios are also presented to demonstrate the capability of the proposed approach.**

I. INTRODUCTION

In target tracking the objective is to estimate an unknown and time varying number of targets and their trajectories from sensor data [1]. The tracking is often performed on data that have been preprocessed into point measurements or detections. Compressing the data image into a finite set of points is efficient in terms of memory as well as computational requirements, and is very effective for a wide range of applications. However, this approach may not be adequate for applications with low signal to noise ratio (SNR) as the information loss incurred in the detection process becomes significant, leading to poor detection probability and large number of false observations. Consequently it is necessary to make use of all information contained in the image(s) to improve tracking performance.

The idea of track-before-detect (TBD), or tracking without detection, and its importance in low SNR radar applications was first investigated in [2], [3]. Since then a number of TBD techniques and applications have been studied [4], [5], [6], [7], [8], [9], [10], [11], [12], [13]. A number of tracking without detection techniques have also appeared in the computer vision literature, see for example [14] and references therein. The multi-Bernoulli RFS approach proposed in [12] is a provably Bayes optimal approach to multi-target filtering on image data, which has been successfully demonstrated on TBD [13], and visual tracking [14], [15]. However, this approach is not, in principle, a multi-target tracker because it rests on the premise that targets are indistinguishable. While the term multi-target filtering is often used interchangeably with multi-target tracking, there is a subtle difference. In multi-target tracking, we are also interested in the trajectories of the targets.

Inspired by the results in [12], and [16], in this paper we propose a labeled RFS solution to multi-target TBD for radar signals. Specifically we use the family of generalized labeled multi-Bernoulli distribution introduced [16] to model the multi-target states and a separable measurement likelihood function [12] to model the pre-detection radar signal. The separability of the measurement likelihood function ensures that the family of generalized labeled multi-Bernoulli distributions is closed under the Bayes recursion. Since the measurement model is non-linear we use a Sequential Monte Carlo (SMC) implementation of the prediction and update step of the Bayes recursion. Simulation results for realistic radar-based TBD scenarios are also presented to verify the capability of the proposed approach. In applications where the separability condition is not guaranteed, the idea of a switch or hybrid likelihood function proposed in [17] can be used to accommodate overlapping targets while preserving the conjugacy of the generalized labeled multi-Bernoulli posterior.

The paper is structured as follows: in section II we recall some definitions and results for labels RFS and review the Bayesian approach to multi-target tracking with labeled RFS. In section III we describe the multi-object TBD likelihood and the proposed multi-target TBD filter. In Section IV we show the achievable performance by means of simulation for realistic radar-based scenarios.

II. BACKGROUND

In essence, an RFS is simply a finite-set-valued random variable. In this paper we use the FISST notion of integration/density[1] to characterize RFSs [1], [19].

A. Labeled RFS

To incorporate target identity, each state $x \in \mathbb{X}$ is augmented with a unique label $\ell \in \mathbb{L}= \{\alpha_i : i \in \mathbb{N}\}$, where $\mathbb{N}$ denotes the set of positive integers and the α_i's are distinct [16].

Definition 1: A *labeled* RFS with state space $\mathbb{X}$ and (discrete) label space $\mathbb{L}$ is an RFS on $\mathbb{X}\times\mathbb{L}$ such that each realization has distinct labels.

Let $\mathcal{L} : \mathbb{X}\times\mathbb{L} \to \mathbb{L}$ be the projection $\mathcal{L}((x,\ell)) = \ell$, then a finite subset set $\mathbf{X}$ of $\mathbb{X}\times\mathbb{L}$ has distinct labels if and only if $\mathbf{X}$ and its labels $\mathcal{L}(\mathbf{X}) = \{\mathcal{L}(\mathbf{x}) : \mathbf{x} \in \mathbf{X}\}$ have the same

[a] Department of Electrical and Computer Engineering, Curtin University, Bentley, WA 6102, Australia. (e-mail: ba-ngu.vo@curtin.edu. au).

[b] Thales Nederland B.V. - Sensors, Hengelo, Nederland. (e-mail: melanie.bocquel@nl.thalesgroup.com)

[c] Maritime Affairs Unit, Institute for the Protection and Security of the Citizen (IPSC), European Commission, Joint Research Centre, Ispra, Italy. (e-mail: francesco.papi@jrc.ec.europa.eu)

[1]The FISST density is equivalent to a probability density relative to an unnormalized distribution of a Poisson RFS (see [18]).

cardinality, i.e. $\delta_{|\mathbf{X}|}(|\mathcal{L}(\mathbf{X})|) = 1$. The function $\Delta(\mathbf{X}) \triangleq \delta_{|\mathbf{X}|}(|\mathcal{L}(\mathbf{X})|)$ is called the *distinct label indicator*.

The unlabeled version of a labeled RFS is obtained by simply discarding the labels. Consequently, the cardinality distribution (the distribution of the number of objects) of a labeled RFS the same as its unlabeled version [16].

For the rest of the paper, single-object states are represented by lowercase letters, e.g. x, $\mathbf{x}$ while multi-object states are represented by uppercase letters, e.g. X, $\mathbf{X}$, symbols for labeled states and their distributions are bolded to distinguish them from unlabeled ones, e.g. $\mathbf{x}$, $\mathbf{X}$, π, etc., spaces are represented by blackboard bold e.g. $\mathbb{X}$, $\mathbb{Z}$, $\mathbb{L}$, $\mathbb{N}$, etc., and the class of finite subsets of a space $\mathbb{X}$ is denoted by $\mathcal{F}(\mathbb{X})$. The integral of a function $\mathbf{f}: \mathbb{X}\times\mathbb{L} \to \mathbb{R}$ is given by

$$\int \mathbf{f}(\mathbf{x})d\mathbf{x} = \sum_{\ell\in\mathbb{L}} \int_{\mathbb{X}} \mathbf{f}((x,\ell))dx.$$

B. Labeled multi-Bernoulli RFS

A labeled multi-Bernoulli RFS $\mathbf{X}$ with state space $\mathbb{X}$, label space $\mathbb{L}$ and (finite) parameter set $\{(r^{(\zeta)}, p^{(\zeta)}) : \zeta \in \Psi\}$, is a multi-Bernoulli RFS on $\mathbb{X}$ augmented with labels corresponding to the successful (non-empty) Bernoulli components, i.e. if the Bernoulli component $(r^{(\zeta)}, p^{(\zeta)})$ yields a non-empty set, then the label of the corresponding state is given by $\alpha(\zeta)$, where $\alpha : \Psi \to \mathbb{L}$ is a 1-1 mapping. The following procedure illustrates how a sample from such a labeled multi-Bernoulli RFS is generated:

Sampling a labeled Multi-Bernoulli RFS

- initialize $\mathbf{X} = \emptyset$;
- for $\zeta \in \Psi$
- sample $u \sim \text{Uniform}[0,1]$;
- if $u \leq r^{(\zeta)}$,
- sample $x \sim p^{(\zeta)}(\cdot)$;
- set $\mathbf{X} = \mathbf{X} \cup \{(x, \alpha(\zeta))\}$;
- end;
- end;

The set of labeled states generated by the above algorithm has (multi-target) density given by [16]

$$\pi(\mathbf{X}) = \Delta(\mathbf{X}) 1_{\alpha(\Psi)}(\mathcal{L}(\mathbf{X})) \left[\Phi(\mathbf{X};\cdot)\right]^{\Psi} \tag{1}$$

where $\Delta(\mathbf{X})$ is the distinct label indicator, $\mathcal{L}(\mathbf{X})$ the set of labels of $\mathbf{X}$, and

$$\Phi(\mathbf{X};\zeta) = \begin{cases} 1 - r^{(\zeta)}, & \text{if } \alpha(\zeta) \notin \mathcal{L}(\mathbf{X}) \\ r^{(\zeta)} p^{(\zeta)}(x), & \text{if } (x, \alpha(\zeta)) \in \mathbf{X} \end{cases}.$$

C. Generalized Labeled Multi-Bernoulli RFS

A generalized labeled multi-Bernoulli RFS is a labeled RFS on $\mathbb{X}\times\mathbb{L}$ distributed according to

$$\pi(\mathbf{X}) = \Delta(\mathbf{X}) \sum_{c\in\mathbb{C}} w^{(c)}(\mathcal{L}(\mathbf{X})) \left[p^{(c)}\right]^{\mathbf{X}} \tag{2}$$

where $\Delta(\mathbf{X})$ is the distinct label indicator, $\mathbb{C}$ is a discrete index set, $w^{(c)}(L)$ and $p^{(c)}$ satisfy

$$\sum_{L\subseteq\mathbb{L}} \sum_{c\in\mathbb{C}} w^{(c)}(L) = 1, \tag{3}$$

$$\int p^{(c)}(x,\ell)dx = 1. \tag{4}$$

A generalized labeled multi-Bernoulli can be interpreted as a mixture of multi-object exponentials. Each term in the mixture (2) consists of a weight $w^{(c)}(\mathcal{L}(\mathbf{X}))$, and a multi-object exponential $\left[p^{(c)}\right]^{\mathbf{X}}$ that depends on the entire multi-object state. The cardinality distribution of a generalized labeled multi-Bernoulli RFS is given by

$$\rho(n) = \sum_{L\in\mathcal{F}_n(\mathbb{L})} \sum_{c\in\mathbb{C}} w^{(c)}(L) \tag{5}$$

It can be easily verified that (5) is indeed a probability distribution, and that the probability density π in (2) integrates to 1. Hence, the RFS defined above is indeed a labeled RFS. Since the multi-object TBD likelihood in eq. (17) is separable, the generalized labeled multi-Bernoulli is conjugate under Bayes update, i.e. if the prior distribution is a generalized labeled multi-Bernoulli, then the posterior distribution is also a generalized labeled multi-Bernoulli.

D. Bayesian Multi-target Filtering

To perform tracking in the Bayes multi-target filtering framework, targets are identified by an ordered pair of integers $\ell = (k,i)$, where k is the time of birth and $i \in \mathbb{N}$, with $\mathbb{N}$ denoting the set of natural numbers, is a unique index to distinguish objects born at the same time. The label space for objects born at time k, denoted as $\mathbb{L}_k$, is then $\{k\}\times\mathbb{N}$. An object born at time k, has state $\mathbf{x} \in \mathbb{X}\times\mathbb{L}_k$. The label space for targets at time k (including those born prior to k), denoted as $\mathbb{L}_{0:k}$, is constructed recursively by $\mathbb{L}_{0:k} = \mathbb{L}_{0:k-1} \cup \mathbb{L}_k$. A multi-object state $\mathbf{X}$ at time k, is a finite subset of $\mathbb{X}\times\mathbb{L}_{0:k}$. Note that $\mathbb{L}_{0:k-1}$ and $\mathbb{L}_k$ are disjoint.

Suppose that at time k, there are $n(k)$ target states $\mathbf{x}_{k,1}, \ldots, \mathbf{x}_{k,n(k)}$, each taking values in the (labeled) state space $\mathbb{X}\times\mathbb{L}$. In the random finite set formulation the set of targets at time k, [19], [1] are treated as the *multi-target state*

$$\mathbf{X}_k = \{\mathbf{x}_{k,1}, \ldots, \mathbf{x}_{k,n(k)}\}.$$

In TBD the multi-target observation at time k is a size vector $z_k = [z_k^{(1)} \ldots z_k^{(m)}]$, where each $z_k^{(i)}$ is a power/image measurement from the radar/camera cell indexed by i.

Let $\pi_k(\cdot|Z_k)$ denotes the *multi-target posterior density* at time k, and $\pi_{k+1|k}$ denotes the *multi-target prediction density* to time k (formally π_k and $\pi_{k+1|k}$ should be written respectively as $\pi_k(\cdot|z_0, ..., z_{k-1}, z_k)$, and $\pi_{k+1|k}(\cdot|z_0, ..., z_k)$, but for simplicity the dependence on past measurements have been omitted). Then, the *multi-target Bayes recursion* propagates π_k in time [19], [1] according to the following

update and prediction

$$\pi_k(\mathbf{X}_k|z_k) = \frac{g_k(z_k|\mathbf{X}_k)\pi_{k|k-1}(\mathbf{X}_k)}{\int g_k(z_k|\mathbf{X})\pi_{k|k-1}(\mathbf{X})\delta\mathbf{X}}, \quad (6)$$

$$\pi_{k+1|k}(\mathbf{X}_{k+1}) = \int \mathbf{f}_{k+1|k}(\mathbf{X}_{k+1}|\mathbf{X}_k)\pi_k(\mathbf{X}_k|z_k)\delta\mathbf{X}_k, \quad (7)$$

where $g_k(\cdot|\cdot)$ is the *multi-target likelihood function* at time k, $\mathbf{f}_{k+1|k}(\cdot|\cdot)$ is the *multi-target transition density*, to time $k+1$, and the integral is a set integral defined for any function $\mathbf{f} : \mathcal{F}(\mathbb{X}\times\mathbb{L}) \to \mathbb{R}$ by

$$\int \mathbf{f}(\mathbf{X})\delta\mathbf{X} = \sum_{i=0}^{\infty} \frac{1}{i!} \int \mathbf{f}(\{\mathbf{x}_1, ..., \mathbf{x}_i\})d(\mathbf{x}_1, ..., \mathbf{x}_i).$$

The multi-target posterior density captures all information on target number, and individual target states [1]. The multi-target likelihood function encapsulates the underlying models for detections and false alarms while the multi-target transition density encapsulates the underlying models of target motions, births and deaths.

For convenience, in what follows we omit explicit references to the time index k, and denote $\mathbb{L} \triangleq \mathbb{L}_{0:k}$, $\mathbb{B} \triangleq \mathbb{L}_{k+1}$, $\mathbb{L}_+ \triangleq \mathbb{L} \cup \mathbb{B}$, $\pi \triangleq \pi_k$, $\pi_+ \triangleq \pi_{k+1|k}$, $g \triangleq g_k$, $\mathbf{f} \triangleq \mathbf{f}_{k+1|k}$.

E. Multi-target Prediction

Given the current multi-object state $\mathbf{X}$, each state $(x, \ell) \in \mathbf{X}$ either continues to exist at the next time step with probability $p_S(x, \ell)$ and evolves to a new state (x_+, ℓ_+) with probability density $f(x_+|x, \ell)\delta_\ell(\ell_+)$, or dies with probability $1 - p_S(x, \ell)$. The set of new targets born at the next time step is distributed according to

$$\mathbf{f}_B(\mathbf{Y}) = \Delta(\mathbf{Y})w_B(\mathcal{L}(\mathbf{Y}))\left[p_B\right]^{\mathbf{Y}} \quad (8)$$

The birth density $\mathbf{f}_B$ is defined on $\mathbb{X} \times \mathbb{B}$ and $\mathbf{f}_B(\mathbf{Y}) = 0$ if $\mathbf{Y}$ contains any element $\mathbf{y}$ with $\mathcal{L}(\mathbf{y}) \notin \mathbb{B}$. The birth model (8) covers both labeled Poisson and labeled multi-Bernoulli. For a labeled multi-Bernoulli birth model:

$$w_B(J) = \prod_{i\in\mathbb{B}(M)} \left(1 - r_B^{(i)}\right) \prod_{\ell\in J} \frac{1_{\mathbb{B}(M)}(\ell)r_B^{(\ell)}}{1 - r_B^{(\ell)}}, \quad (9)$$

$$p_B(x, \ell) = p_B^{(\ell)}(x). \quad (10)$$

The multi-target state at the next time $\mathbf{X}_+$ is the superposition of surviving targets and new born targets. Assuming that targets evolve independently of each other and that births are independent of surviving targets, it was shown in [16] that the multi-target transition kernel is given by

$$\mathbf{f}\left(\mathbf{X}_+|\mathbf{X}\right) = \mathbf{f}_S(\mathbf{X}_+ \cap (\mathbb{X}\times\mathbb{L})|\mathbf{X})\mathbf{f}_B(\mathbf{X}_+ - (\mathbb{X}\times\mathbb{L})) \quad (11)$$

where

$$\mathbf{f}_S(\mathbf{W}|\mathbf{X}) = \Delta(\mathbf{W})\Delta(\mathbf{X})1_{\mathcal{L}(\mathbf{X})}(\mathcal{L}(\mathbf{W}))\left[\Phi(\mathbf{W};\cdot)\right]^{\mathbf{X}}$$

$$\Phi(\mathbf{W};x,\ell) = \begin{cases} p_S(x,\ell)f(x_+|x,\ell), & \text{if } (x_+,\ell) \in \mathbf{W} \\ 1 - p_S(x,\ell), & \text{if } \ell \notin \mathcal{L}(\mathbf{W}) \end{cases}$$

Moreover, the generalized labeled multi-Bernoulli family is closed under the multi-target prediction. In particular, if the prior π is given by (2) the predicted multi-target density is given by

$$\pi_+(\mathbf{X}_+) = \Delta(\mathbf{X}_+)\sum_{c\in\mathbb{C}} w_+^{(c)}(\mathcal{L}(\mathbf{X}_+))\left[p_+^{(c)}\right]^{\mathbf{X}_+} \quad (12)$$

where explicit expressions for $w_+^{(c)}(L)$, $p_+^{(c)}(x,\ell)$, $p_S^{(c)}(x,\ell)$, $\eta_S^{(c)}(\ell)$, $w_S^{(c)}(J)$, and $q_S^{(c)}(\ell)$ can be found in [16]. Eq. (12) explicitly describes how to calculate the parameters of the predicted multi-object density from the parameters of the prior multi-object density.

III. Labeled RFS TBD

In this section we describe the multi-target TBD measurement model and show that the family of δ-generalized labeled multi-Bernoulli distributions is conjugate with respect to this separable likelihood function.

A. Measurement likelihood function

We now describe a multi-target observation model for TBD. Target returns measured by the radar are assumed to fluctuate according to the Swerling return amplitude fluctuation models [20]. Here the Swerling fluctuation models are incorporated into the likelihood function of the filter, to account for the target return fluctuations. A target $\mathbf{x} \in \mathbf{X}$, at time k, illuminates a set of cells $C(\mathbf{x})$. A radar positioned at the Cartesian origin collects a measurement $z = [z^{(1)} \dots z^{(m)}]$, which consists of the power signal for all m range-Doppler-bearing cells:

$$z^{(i)} = |z_A^{(i)}|^2 \quad (13)$$

where $z_A^{(i)}$ is the complex signal in cell i, i.e.

$$z_A^{(i)} = \sum_{\mathbf{x}\in\mathbf{X}:i\in C(\mathbf{x})} A(\mathbf{x})h_A(\mathbf{x}) + w \quad (14)$$

Here,

- w is a m-dimensional zero-mean, white complex Gaussian noise with variance σ_w^2.
- $h_A(\mathbf{x}) = \left[[h_A(\mathbf{x})]^{(1)} \dots [h_A(\mathbf{x})]^{(m)}\right]$ represents the point spread function at a target of state $\mathbf{x}$, i.e.

$$[h_A(\mathbf{x})]^{(i)} = \exp\left(-\frac{(r_i - r(\mathbf{x}))^2}{2R} - \frac{(d_i - d(\mathbf{x}))^2}{2D} - \frac{(b_i - b(\mathbf{x}))^2}{2B}\right) \quad (15)$$

  R, D and B are constants related to the radar cell resolution, and $r(\mathbf{x})$, $d(\mathbf{x})$, and $b(\mathbf{x})$ are the target coordinates in the measurement space, and r_i, d_i, b_i are the bin centroids.
- $A(\mathbf{x})$ is the complex echo of target $\mathbf{x}$, i.e.

$$A(\mathbf{x}) = \bar{A}(\mathbf{x})e^{i\theta} + a(\mathbf{x}) \quad (16)$$

  with $\bar{A}(\mathbf{x})$ a known amplitude, θ an unknown phase uniformly distributed in $[0, 2\pi)$, and $a(\mathbf{x})$ a zero-mean complex Gaussian variable with variance $\sigma_{a(\mathbf{x})}^2$.

Let the measurement likelihood in cell i in the presence of a target with state $\mathbf{x}$ be denoted by $\phi^{(i)}(z^{(i)}|\mathbf{x})$, and the likelihood under the hypothesis of no targets be $\varphi^{(i)}(z^{(i)})$.

Since conditioned on the multi-target state $\mathbf{X}$, the measurement values in the cells are independently distributed, the multi-target likelihood of z is the product over all cells, i.e.

$$g(z|\mathbf{X}) = f(z) \prod_{\mathbf{x}\in\mathbf{X}} \gamma_z(\mathbf{x}) \tag{17}$$

where,

$$f(z) = \prod_{i=1}^{m} \varphi^{(i)}(z^{(i)}) \tag{18}$$

$$\gamma_z(\mathbf{x}) = \prod_{i\in C(\mathbf{x})} \frac{\phi^{(i)}(z^{(i)}|\mathbf{x})}{\varphi^{(i)}(z^{(i)})} \tag{19}$$

Under the assumption of a non-fluctuating target model (Swerling 0), the multi-target observation likelihood $\phi^{(i)}(z^{(i)}|\mathbf{x})$ is a non-central chi-squared distribution and reduces to an exponential distribution if $z^{(i)}$ only contains clutter noise and thermal noise. In fact, in this case the complex echo of the target j is modeled by:

$$A(\mathbf{x}) = \bar{A}(\mathbf{x})e^{i\theta}, \quad \theta \in [0, 2\pi) \tag{20}$$

Let $\Sigma_{h^{(i)}} := \sum_{\mathbf{x}\in\mathbf{X}:i\in C(\mathbf{x})} A(\mathbf{x})h_A(\mathbf{x})$ for notational convenience, then the power signal for cell i is given by:

$$\begin{aligned} z^{(i)} &= |\Sigma_{h^{(i)}} e^{i\theta} + w^{(i)}|^2 \\ &= \left(\Sigma_{h^{(i)}} \cos(\theta) + \Re(w^{(i)})\right)^2 + \left(\Sigma_{h^{(i)}} \sin(\theta) + \Im(w^{(i)})\right)^2 \\ &= U_R^2 + U_I^2 \end{aligned}$$

where $U_R \sim N(\Sigma_{h^{(i)}}\cos(\theta), \sigma^2_{w^{(i)}}/2)$ and $U_I \sim N(\Sigma_{h^{(i)}}\sin(\theta), \sigma^2_{w^{(i)}}/2)$ are statistically independent normal random variables. Then $\sqrt{U_R^2 + U_I^2}$ has a Ricean distribution, and reduces to a Rayleigh distribution when $\Sigma_{h^{(i)}} = 0$. Thus, the measurement likelihood is given by:

$$\phi^{(i)}(z^{(i)}|\mathbf{x}) = \frac{1}{\sigma^2_{w^{(i)}}} \exp\left(-\frac{z^{(i)} + \Sigma_{h^{(i)}}}{\sigma^2_{w^{(i)}}}\right) I_0\left(\sqrt{\frac{4z^{(i)}\Sigma_{h^{(i)}}}{\sigma^2_{w^{(i)}}}}\right) \tag{21}$$

$$\varphi^{(i)}(z^{(i)}) = \frac{1}{\sigma^2_{w^{(i)}}} \exp\left(-\frac{z^{(i)}}{\sigma^2_{w^{(i)}}}\right) \tag{22}$$

where $I_0(\cdot)$ is the Bessel function defined as:

$$I_0(x) := \sum_{j=0}^{\infty} \frac{\left(x^2/4\right)^j}{j!\Gamma(j+1)} \tag{23}$$

B. Conjugacy and Generalized Labeled Multi-Bernoulli TBD filter

One of the first known RFS conjugate priors with respect to a separable likelihood function is the (unlabeled) multi-Bernoulli family [12]. Indeed the multi-Bernoulli filter (for image data) was based on this result.

Since the generalized labeled multi-Bernoulli is a generalization of the (unlabeled) multi-Bernoulli family, it follows that the generalized labeled multi-Bernoulli is also a conjugate prior with respect to a separable likelihood function. Moreover, if the prior π is given by (2) then posterior multi-target density is given by

$$\pi(\mathbf{X}|z) \propto \Delta(\mathbf{X}) \sum_{c\in\mathbb{C}} w^{(c)}(\mathcal{L}(\mathbf{X})) \left[p^{(c)}(\cdot|z)\right]^{\mathbf{X}} \tag{24}$$

where

$$w_z^{(c)}(L) = [\eta_z]^L w^{(c)}(L) \tag{25}$$

$$p^{(c)}(x,\ell|z) = \frac{p^{(c)}(x,\ell)\gamma_z(x,\ell)}{\left\langle p^{(c)}(\cdot,\ell), \gamma_z(\cdot,\ell)\right\rangle}. \tag{26}$$

$$\eta_z(\ell) = \left\langle p^{(c)}(\cdot,\ell), \gamma_z(\cdot,\ell)\right\rangle \tag{27}$$

The generalized labeled multi-Bernoulli TBD filter consists of a prediction step and update step given respectively by (12) and (24).

IV. Numerical example

In this section, the performance of the proposed generalized labeled multi-Bernoulli TBD filter is tested on simulation in realistic radar based surveillance scenarios. We implemented the proposed TBD filter via SMC methods.

A. System Dynamics

The (single-target) state vector $x_k = [\ \tilde{x}_k^T, \rho_k\ ]^T$, at time k, comprises the planar position and velocity $\tilde{x}_k = [\ p_{x,k}, \dot{p}_{x,k}, p_{y,k}, \dot{p}_{y,k}\ ]^T$, in 2D Cartesian coordinates, respectively, and $\rho_k \in R$ is the unknown modulo of the target complex amplitude. A Nearly Constant Velocity (NCV) model is used to describe the target dynamics, while a zero-mean Gaussian random walk is used to model the fluctuations in time of the target complex amplitude, i.e.,

$$x_{k+1} = F\ x_k + v_k, \quad v_k \sim \mathcal{N}(0; Q) \tag{28}$$

where v_k is a zero-mean Gaussian noise, T_s the radar sampling time, and the matrices are defined as:

$$F = \text{diag}(F_1, F_1, 1), \quad F_1 = \begin{bmatrix} 1 & T_s \\ 0 & 1 \end{bmatrix} \tag{29}$$

$$Q = \text{diag}(a_x Q_1, a_y Q_1, a_\rho T_s), \quad Q_1 = \begin{bmatrix} \frac{T_s^3}{3} & \frac{T_s^2}{2} \\ \frac{T_s^2}{2} & T_s \end{bmatrix} \tag{30}$$

where a_x and a_y determine the process noise intensity for the motion, and a_ρ describes the amplitude fluctuation. The parameters used in simulation are reported in table I.

B. Simulation Results

We considered 2 slightly different scenarios as depicted in figs. 1 and 2, where we report the targets trajectories (black lines) along with the results for one realization of the tracking problem (blue circles). Case 1 shows a maximum of 4 targets moving inside the surveillance region with an average speed of $15m/\sec$ and an SNR of $13dB$, while in Case 2 there are at most 3 targets with an average speed of $20m/\sec$ a lower SNR of $10dB$. As an example for , in fig. 3 we depicted the received data for Case 2 in the Doppler bin $[10, 12)\ m/\sec$ at time step $k = 10$. Even though from the data there seems to be multiple targets, only target 3 is

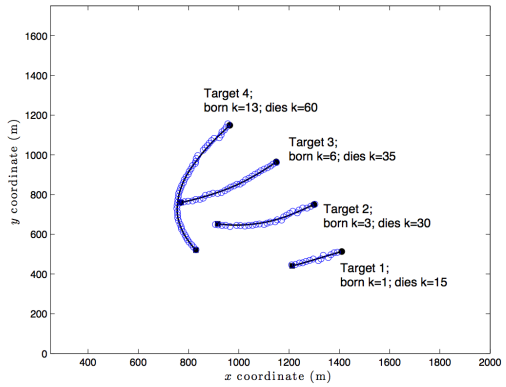

Fig. 1. Scenario 1: a maximum of 4 targets moving inside the surveillance region with an average speed of $15m/\sec$ and an SNR of $13dB$.

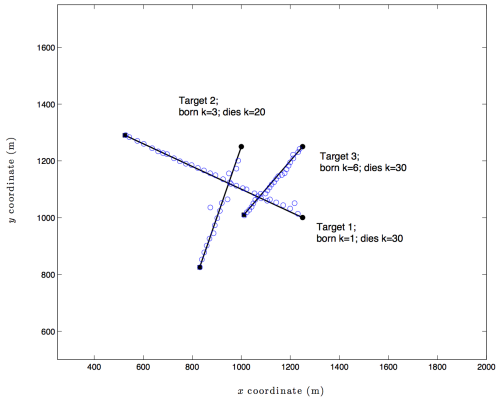

Fig. 2. Scenario 2: a maximum of 3 targets moving inside the surveillance region with an average speed of $20m/\sec$ and an SNR of $10dB$.

included in this Doppler bin. The birth model is a multi-Bernoulli labeled RFS with birth positions centered about the initial target states and having a position uncertainty of $20m$ and a velocity uncertainty of $15m/\sec$.

A radar positioned at the Cartesian origins collects the reflected target power with a sampling interval T_s of $1\sec$. In both cases we considered a realistic radar resolution of $10m$ in range, $2m/\sec$ in Doppler, and $1\deg$ in azimuth.

In figs. 4 and 5 we report the estimated target number, averaged over 100 Monte Carlo trials. We chose the mode of the cardinality distribution as the estimate of the number of targets, since it appears to be more stable than the conditional mean. From the figures, it is immediate to verify that apart from a small time delay, the proposed approach is able to effectively estimate the time-varying target number. In figs. 6 and 7 we report the average optimal subpattern assignment (OSPA) distance [21] evaluated using the Euclidean distance and two different cutoff parameters $c = 10m$ and $c = 50m$. Again, the figure verifies that the proposed approach can effectively tackle the multi-target TBD tracking problem.

TABLE I
PARAMETERS USED IN SIMULATION

Parameter	Symbol	Value
Signal to Noise Ratio	SNR	$\{13, 10\}dB$
Range Quant Size	R	$10m$
Doppler Bin Size	D	$2m/\sec$
Beam Spacing	B	$1\deg$
radar Sampling Time	T_s	$1\sec$
Average Target Speed	v	$\{15, 20\}m/\sec$
Maximum x-acceleration	a_x	$1m/\sec^2$
Maximum y-acceleration	a_y	$1m/\sec^2$
Number of particles	N	$\{500\}$
Maximun n° of targets	n_{max}	8
Number of components	N_c	900
n° of best-ranked hypotheses	N_h	450
Min. n° of components $\forall\ n_k$	N_{min}	40

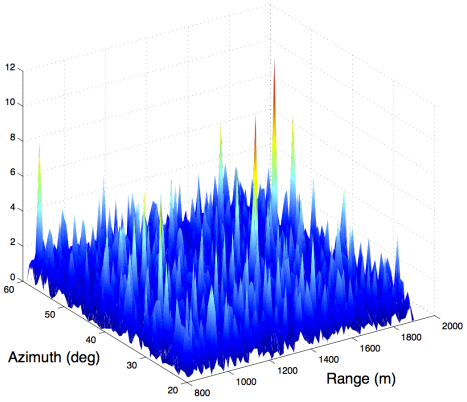

Fig. 3. Scenario 2: received data for the Doppler bin $[10, 12)\ m/\sec$ at time $k = 10$. Only target 3 is included in this Doppler bin.

V. CONCLUSIONS AND FUTURE WORK

In this paper we have presented a labeled RFS solution to the multi-target TBD problem. To the best of our knowledge this is the first provably Bayes optimal approach to multi-target tracking using image data. Simulation results based on realistic scenarios showed encouraging performance, and demonstrated the potential power of the proposed approach.

Given the wide range of applicability of multi-target tracking and the great number of engineering problems related to recursive multi-object estimation, many questions remain open. For instance, more efficient particle implementations and the development of solutions for specific aspects of a tracking system are two directions for future research [22].

VI. ACKNOWLEDGMENTS

This work is supported by a project from the ISR Division of DSTO, and by the Australian Research Council under schemes DE120102388 and FT0991854.

The third author is supported by the EU's Seventh Framework Programme, grant agreement n^o 238710, MC IMPULSE project: https://mcimpulse.isy.liu.se

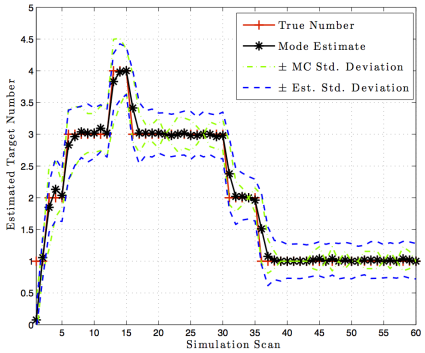

Fig. 4. Scenario 1: Cardinality mode estimate of the target number ± standard deviation over 100 Monte Carlo trials.

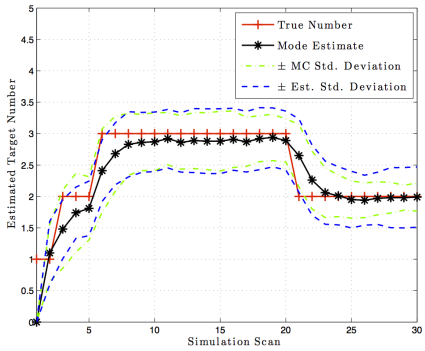

Fig. 5. Scenario 2: Cardinality mode estimate of the target number ± standard deviation over 100 Monte Carlo trials.

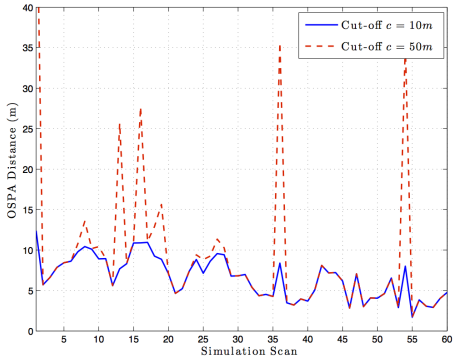

Fig. 6. Scenario 1: Average OSPA distance for $c = \{10, 50\}m$

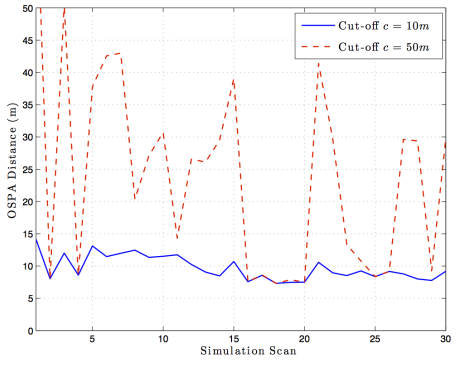

Fig. 7. Scenario 2: Average OSPA distance for $c = \{10, 50\}m$

REFERENCES

[1] R.P.S. Mahler. *Statistical Multisource-Multitarget Information Fusion*. Artech House, 2007.

[2] D.J. Salmond and H. Birch. A particle filter for track-before-detect. *Proc. American Control Conference*, 5:3755–3760, June 2001, Arlington, Va, USA.

[3] Y. Boers and J.N. Driessen. Particle Filter based Detection for Tracking. *Proc. of the 2001 American Control Conference*, pages 4393–4397, 2001.

[4] S. Tonissen and Y. Bar-Shalom. Maximum likelihood track-before-detect with fluctuating target amplitude. *IEEE Transactions on Aerospace and Electronic Systems*, 3:796–808, 1998.

[5] D. Orlando, L. Venturino, M. Lops, and G. Ricci. Track-before-detect strategies for stap radars. *IEEE Transactions on Signal Processing*, 58(2):933–938, 2010.

[6] M. Fallon and S. Godsill. Acoustic source localization and tracking using track before detect. *IEEE Transactions on Audio, Speech and Language Processing*, 18(6):1228–1242, 2010.

[7] S. Buzzi, M. Lops, and L. Venturino. Track-before-detect procedures for early detection of moving target from airborne radars. *IEEE Transactions on Aerospace and Electronic Systems*, 41(3):937–954, 2005.

[8] Y. Boers and J. N. Driessen. Particle Filter Track-Before-Detect Application Using Hard Inequality Constraints. *IEEE Transactions on Aerospace and Electronic Systems*, 41(4):1483–1489, 2005.

[9] T. Wettergren. Performance of search via track-before-detect for distributed sensor networks. *IEEE Transactions on Aerospace and Electronic Systems*, 44(1):314–325, 2008.

[10] S. Davies, M. Rutten, and B. Cheung. Comparison of Detection Performance for several Track-Before-Detect algorithms. *EURASIP Journal on Advances in Signal Processing*, 2008(1):Article 41, 2008.

[11] S. Saha, Y. Boers, H. Driessen, P.K. Mandal, and A. Bagchi. Particle filter based map state estimation: A comparison. *Proc. of the 12th Int. Conf. on Information Fusion*, Seattle, WA, USA 2009.

[12] B.-N. Vo, B.-T. Vo, N.T. Pham, and D. Suter. Joint Detection and Estimation of Multiple Objects From Image Observations. *IEEE Transactions on Signal Processing*, 61(13):3460–3475, 2010.

[13] J. Wong, B.-T. Vo, B.-N. Vo, and R. Hoseinnezhad. Multi-Bernoulli based Track-Before-Detect with Road Constraints. *Proc. 15th Annual Conf. Information Fusion*, July 2012, Singapore.

[14] R. Hoseinnezhad, B.-N. Vo, D. Suter, and B.-T. Vo. Visual tracking of numerous targets via multi-Bernoulli filtering of image data. *Pattern Recognition*, 45(10):3625–3635, 2012.

[15] R. Hoseinnezhad, B.-N. Vo, and B.-T. Vo. Visual Tracking in Background Subtracted Image Sequences via Multi-Bernoulli Filtering. *IEEE Transactions on Signal Processing*, 61(2):392–397, 2013.

[16] B.-T. Vo and B.-N. Vo. Labeled Random Finite Sets and Multi-Object Conjugate Priors. *IEEE Transactions on Signal Processing*, 61(13), July 2013.

[17] D.-Y. Kim, B.-T. Vo, and B.-N. Vo. Data Fusion in 3D Vision Using a RGB-D Data Via Switching Observation Model and Its Application to People Tracking. *Proc. Int. Conf. Control Aut. & Info Sciences*, Vietnam, November 2013.

[18] B.-N. Vo, S. Singh, and A. Doucet. Sequential Monte Carlo methods for Multi-target filtering with Random Finite Sets. *IEEE Transactions on Aerospace and Electronic Systems*, 41(4):1224–1245, 2005.

[19] R. Mahler. Multi-target Bayes filtering via first-order multi-target moments. *IEEE Trans. Aerospace & Electronic Systems*, 39(4):1152–1178, 2003.

[20] M. Skolnik. *Introduction to Radar Systems*. McGraw Hill, 2003.

[21] D. Schuhmacher, B.-T. Vo, and B.-N. Vo. A consistent metric for performance evaluation of multi-object filters. *IEEE Trans. Signal Processing*, 56(8):3447–3457, 2008.

[22] M. Bocquel. *Random Finite Sets in Multi-target Tracking: Efficient Sequential MCMC implementation*. PhD thesis, Faculty of Electrical Engineering, Mathematics and Computer Science, University of Twente, Manuscript submitted to committee, October 2013.